Mineralogical Magazine (2024), **88**, 49–60
doi:10.1180/mgm.2023.85

CAMBRIDGE UNIVERSITY PRESS

Article

A new mineral cuprodobrovolskyite $Na_4Cu(SO_4)_3$ from the Tolbachik volcano (Kamchatka, Russia) and relationships in the family of natural anhydrous Na–Cu sulfates

Nadezhda V. Shchipalkina[1], Igor V. Pekov[1], Natalia N. Koshlyakova[1], Dmitry I. Belakovskiy[2], Natalia V. Zubkova[1], Atali A. Agakhanov[2], Sergey N. Britvin[3] and Maria A. Nazarova[4]

[1]Faculty of Geology, Moscow State University, Vorobievy Gory, Moscow, 119991 Russia; [2]Fersman Mineralogical Museum of the Russian Academy of Sciences, Leninsky Prospekt 18-2, Moscow, 119071 Russia; [3]Department of Crystallography, St Petersburg State University, University Embankment 7/9, 199034 St Petersburg, Russia; and [4]Institute of Volcanology and Seismology, Far Eastern Branch of Russian Academy of Sciences, Piip Boulevard 9, 683006 Petropavlovsk-Kamchatsky, Russia

Abstract

A new mineral cuprodobrovolskyite, ideally $Na_4Cu(SO_4)_3$, was found in sublimates of the Arsenatnaya fumarole at the Second scoria cone of the Northern Breakthrough of the Great Tolbachik Fissure Eruption, Tolbachik volcano, Kamchatka, Russia. It is associated with petrovite, saranchinaite, euchlorine, krasheninnikovite, langbeinite, calciolangbeinite, anhydrite, sanidine, tenorite and hematite. Cuprodobrovolskyite occurs as coarse hexagonal tabular or equant, typically skeletal crystals up to 1 mm and their clusters or crusts up to 1.5 cm × 2.5 cm in area. The mineral is transparent, light blue or greenish-bluish to almost colourless with vitreous lustre. Cuprodobrovolskyite is optically uniaxial (+) with $\omega = 1.509(3)$ and $\epsilon = 1.528(3)$. The empirical formula calculated on the basis of 12 O apfu is $(Na_{3.64}K_{0.09}Pb_{0.03})_{\Sigma 3.76}(Cu_{0.51}Ca_{0.22}Mg_{0.16}Zn_{0.07}Al_{0.01}Mn_{0.01})_{\Sigma 0.98}S_{3.04}O_{12}$. The unit-cell parameters of cuprodobrovolskyite calculated from the powder X-ray diffraction data are: $a = 15.702(2)$, $c = 22.017(5)$ Å, $V = 4701.0(2)$ Å^3, space group $R3$ and $Z = 18$. The crystal structure was studied using the Rietveld method, $R_p = 0.0246$, $R_{wp} = 0.0325$, $R_1 = 0.0521$ and $wR_2 = 0.0770$. Cuprodobrovolskyite is an isostructural analogue of dobrovolskyite $Na_4Ca(SO_4)_3$ with Cu prevailing over Ca. One of the main features of cuprodobrovolskyite is Cu^{2+} in 7-fold coordination. On the basis of relationships with saranchinaite $Na_2Cu(SO_4)_2$ and petrovite $Na_{12}Cu_2(SO_4)_8$ in the Arsenatnaya fumarole and the results of heating experiments, cuprodobrovolskyite is considered as the highest-temperature phase among anhydrous Na–Cu sulfate minerals.

Keywords: cuprodobrovolskyite; dobrovolskyite; saranchinaite; petrovite; new mineral; anhydrous alkali-copper sulfate; crystal structure; fumarole sublimates; Tolbachik volcano

(Received 13 April 2023; accepted 31 October 2023; Accepted Manuscript published online: 13 November 2023; Associate Editor: David Hibbs)

Introduction

The anhydrous sodium–copper sulfates are of interest for mineralogists, geochemists, physicists and materials scientists because of their genetic significance in postvolcanic fumarolic systems and perspective magnetic and non-linear optic properties (Kovrugin *et al.*, 2019; Borisov *et al.*, 2021; Siidra *et al.*, 2021a, 2021b, 2021c; Singh *et al.*, 2022). These papers have shown, for example, that the eldfellite-type phase $NaFe(SO_4)_2$ is characterised by 8 mAh/g of reversible capacity with a discharge voltage of 3.0 V and that the synthetic analogue of saranchinaite can be considered as a high voltage cathode (4.84 V *vs* Li^+/Li^0). However, natural samples of such sulfates and their synthetic counterparts tend to have narrow fields of thermodynamic stability and are affected by different transformations including hydration. Thus, each novel natural Na–Cu sulfate sheds a light on formation conditions and crystal chemistry of these types of compounds.

All anhydrous Na–Cu sulfates discovered recently in Nature are endemics of active fumaroles of the Tolbachik volcano (Kamchatka, Russia), namely puninite $Na_2Cu_3O(SO_4)_3$ (Siidra *et al.*, 2017), saranchinaite $Na_2Cu(SO_4)_2$ (Siidra *et al.*, 2018), petrovite $Na_{12}Cu_2(SO_4)_8$ (Filatov *et al.*, 2020), and the mineral described here, cuprodobrovolskyite $Na_4Cu(SO_4)_3$. This latter mineral differs from others in stoichiometry, symmetry, crystal structure and physical properties.

Cuprodobrovolskyite (Cyrillic: купродобровольскиит) is named as an analogue of dobrovolskyite $Na_4Ca(SO_4)_3$ (Shablinskii *et al.*, 2021) with copper prevailing over calcium. Both the new mineral and its name (symbol Cdvo) have been approved by the Commission on New Minerals, Nomenclature and Classification of the International Mineralogical Association (IMA No. 2022-061, Shchipalkina *et al.*, 2023b). The type specimen is deposited in the

Corresponding author: Nadezhda V. Shchipalkina; Email: estel58@yandex.ru
Cite this article: Shchipalkina N.V., Pekov I.V., Koshlyakova N.N., Belakovskiy D.I., Zubkova N.V., Agakhanov A.A., Britvin S.N. and Nazarova M.A. (2024) A new mineral cuprodobrovolskyite $Na_4Cu(SO_4)_3$ from the Tolbachik volcano (Kamchatka, Russia) and relationships in the family of natural anhydrous Na–Cu sulfates. *Mineralogical Magazine* **88**, 49–60. https://doi.org/10.1180/mgm.2023.85

systematic collection of the Fersman Mineralogical Museum of the Russian Academy of Sciences, Moscow, Russia with catalogue number 98046.

Occurrence, morphology and physical properties

The specimens with the new mineral were collected by us in July 2021 at the Arsenatnaya fumarole located at the summit of the Second scoria cone of the Northern Breakthrough of the Great Tolbachik Fissure Eruption 1975–1976, Tolbachik volcano, Kamchatka. This active, high-temperature oxidising-type fumarole is famous as the type locality of more than sixty new mineral species. Its general description is given by Pekov *et al.* (2018) and Shchipalkina *et al.* (2020b). The specimens with cuprodobrovolskyite were collected in fumarolic pockets with temperatures of 350–400°C (the temperature was measured with a chromel–alumel thermocouple during sampling).

Cuprodobrovolskyite is a typical fumarolic mineral. We believe that it was deposited directly from the gas phase as a volcanic sublimate at temperatures not lower than 400°C. Minerals associated closely with cuprodobrovolskyite are petrovite, saranchinaite, euchlorine, krasheninnikovite, langbeinite, calciolangbeinite, anhydrite, sanidine, tenorite and hematite.

Cuprodobrovolskyite occurs as two morphological varieties: (1) coarse hexagonal tabular or equant, typically skeletal crystals up to 1 mm and their clusters or open-work crusts (Figs 1a and 2) up to 5 mm across; and (2) massive crusts, typically interrupted, up to 1.5 cm × 2.5 cm in area and up to 1 mm thick, with a 'glazed' surface (Fig. 1b) which cover basalt scoria altered by fumarolic gas. Cuprodobrovolskyite crystals and crusts contain abundant lamellar and irregular shaped ingrowths of saranchinaite; on the surface, these ingrowths look like grooves (Fig. 2). The relationship between saranchinaite and the host cuprodobrovolskyite is shown in Fig. 3. Other sulfates (petrovite, langbeinite and calciolangbeinite) also form intimate intergrowths with cuprodobrovolskyite.

Cuprodobrovolskyite is transparent, light blue or greenish-bluish to almost colourless. The streak is white. The lustre is vitreous. The Mohs' hardness is *ca*. 3. The mineral is brittle, cleavage or parting was not observed. The density could not be determined correctly owing to several intergrown minerals, represented

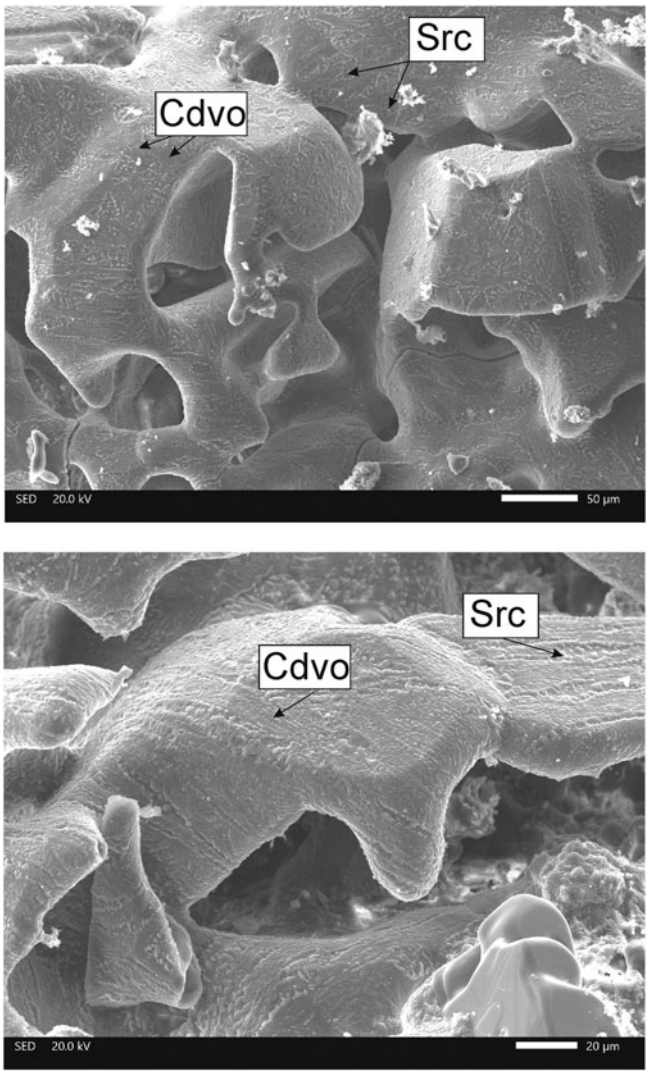

Figure 2. Sulfate crusts consisting of coarse skeletal cuprodobrovolskyite (Cdvo) crystals with ingrowths of saranchinaite (Src). The mineral symbols are given after Warr (2021). Scanning electron microscopy (SEM) images, SE mode. Holotype specimen, # 98046.

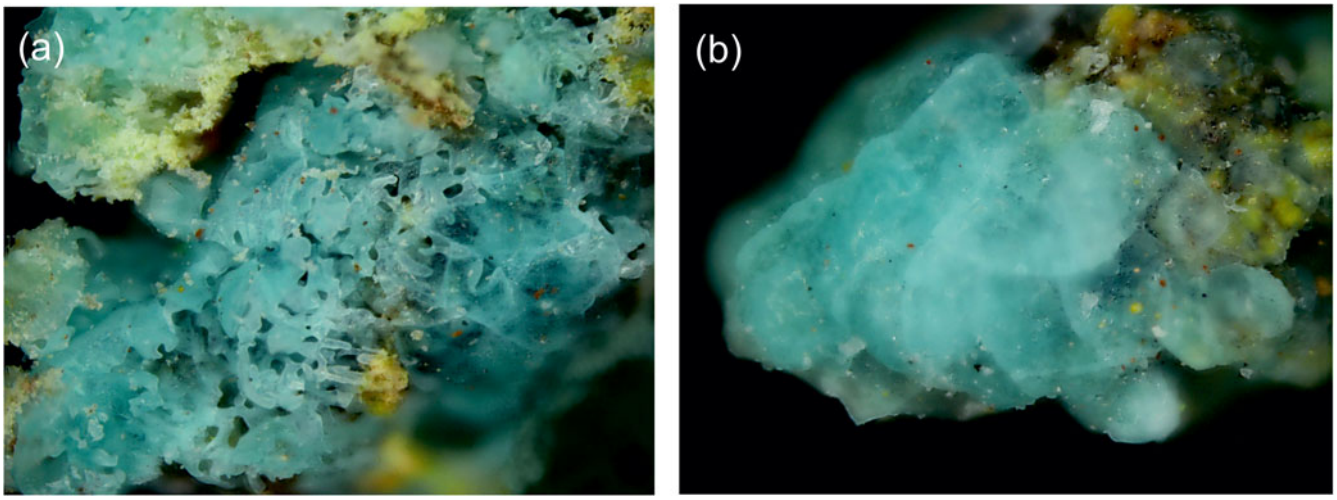

Figure 1. Light blue crusts of cuprodobrovolskyite: (a) open-work crust consisting of coarse skeletal crystals, (b) massive crust. Field of view, width – 1 mm (both images). Holotype specimen, # 98046.

https://doi.org/10.1180/mgm.2023.85 Published online by Cambridge University Press

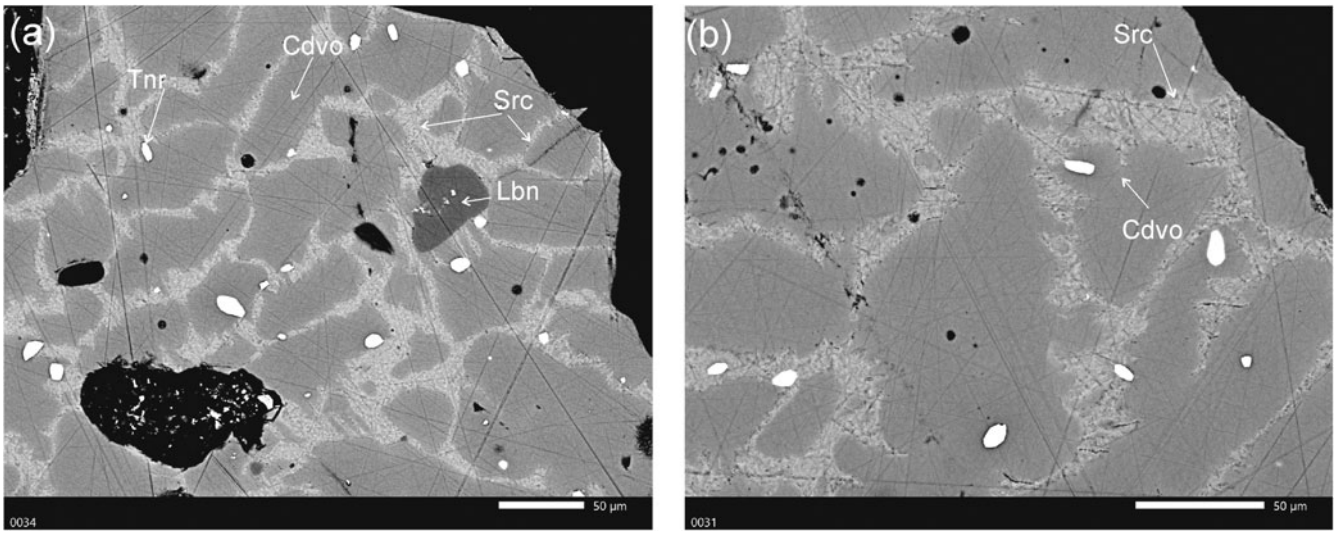

Figure 3. Crystals of cuprodobrovolskyite (Cdvo) with ingrowths (probably relics) of saranchinaite (Src); Tnr – tenorite and Lbn – langbeinite. Polished sections, SEM images, BSE mode. Holotype specimen, # 98046.

mainly by saranchinaite. The density calculated using the empirical formula is 2.783 g cm^{-3}.

Cuprodobrovolskyite is optically uniaxial (+) with $\omega = 1.509(3)$ and $\varepsilon = 1.528(3)$ (589 nm). Under the microscope in plane polarised transmitted light cuprodobrovolskyite is colourless and non-pleochroic. The Gladstone-Dale compatibility index is −0.043 (good).

Methods and results

Chemical composition

The chemical composition of cuprodobrovolskyite was studied using an electron microprobe. The analyses were carried out with a JEOL JXA-8230 (WDS mode) at the Laboratory of Analytical Techniques of High Spatial Resolution, Dept. of Petrology, Moscow State University. The operating conditions included an accelerating voltage of 20 kV and beam current of 20 nA; the beam was rastered on an area 4 μm × 4 μm. The data reduction was carried out using the INCA Energy 300 software package. The following standards were used for quantitative analysis: diopside (Mg), metal Cu (Cu), ZnS (Zn), anorthite (Ca and Al), PbTe (Pb), $SrSO_4$ (Sr) and pyrite (S). Contents of other elements with atomic numbers higher than carbon are below detection limits.

The chemical composition of cuprodobrovolskyite is given in Table 1. The averaged empirical formula of the holotype specimen calculated on the basis of 12 O atoms per formula unit (apfu) is $(Na_{3.64}K_{0.09}Pb_{0.03})_{\Sigma 3.76}(Cu_{0.51}Ca_{0.22}Mg_{0.16}Zn_{0.07}Al_{0.01}Mn_{0.01})_{\Sigma 0.98}S_{3.04}O_{12}$. The simplified formula is $Na_4(Cu,Ca,Mg,Zn)(SO_4)_3$. The ideal formula $Na_4Cu(SO_4)_3$ requires Na_2O 27.88, CuO 17.94, SO_3 54.18, total 100 wt.%.

Raman spectroscopy

The Raman spectra of cuprodobrovolskyite and, for comparison, dobrovolskyite, saranchinaite and petrovite (Fig. 4) were recorded using an EnSpectr R532 spectrometer with a green laser (532 nm) at room temperature. The output power of the laser beam was ~7 mW. The spectrum was processed using the EnSpectr expert

Table 1. Chemical composition of cuprodobrovolskyite from the Arsenatnaya fumarole: holotype (#1) and other specimens (##2, 3) and cuprodobrovolskyite samples after annealing (##4, 5).

Component	1*	2	3	4	5
Wt.%					
Na_2O	25.69 (24.80–26.38)	24.31	25.60	25.43	26.80
K_2O	0.92 (0.84–1.06)	3.60	4.71	1.04	1.09
Rb_2O	0.02 (0.00–0.11)	-	-	-	-
CaO	2.83 (2.40–3.46)	4.80	1.31	4.32	4.26
MgO	1.43 (1.27–1.56)	0.57	-	1.38	1.27
MnO	0.17 (0.11–0.24)	0.25	-	0.29	0.25
CuO	9.33 (8.63–9.61)	8.51	9.96	7.49	7.37
ZnO	1.33 (1.12–1.51)	0.73	0.56	0.19	0.25
SrO	0.03 (0.09–0.10)	0.15	0.16	-	-
PbO	1.50 (1.95–2.12)	-		2.09	1.85
Al_2O_3	0.09 (0.21–0.42)	0.18	0.06	-	-
SO_3	55.36 (54.84–55.94)	55.93	55.67	56.20	56.68
Total	99.55	99.03	98.03	98.43	100.42
Formula coefficients calculated on the basis of 12 O atoms					
Na	3.64	3.43	3.67	3.58	3.70
K	0.09	0.33	0.44	0.10	0.10
Rb	0.00	-	-	-	-
Ca	0.22	0.37	0.10	0.34	0.33
Mg	0.16	0.06	-	0.15	0.16
Mn	0.01	0.02	-	0.02	0.02
Cu	0.51	0.47	0.55	0.41	0.40
Zn	0.07	0.04	0.03	0.01	0.01
Sr	0.00	0.01	0.01	-	-
Pb	0.03	-	-	0.04	0.04
Al	0.01	0.02	0.01	-	-
S	3.04	3.04	3.08	3.07	3.05

*Averaged for 10 spot analyses, ranges are in parentheses; '–' means the content was below the detection limit.

https://doi.org/10.1180/mgm.2023.85 Published online by Cambridge University Press

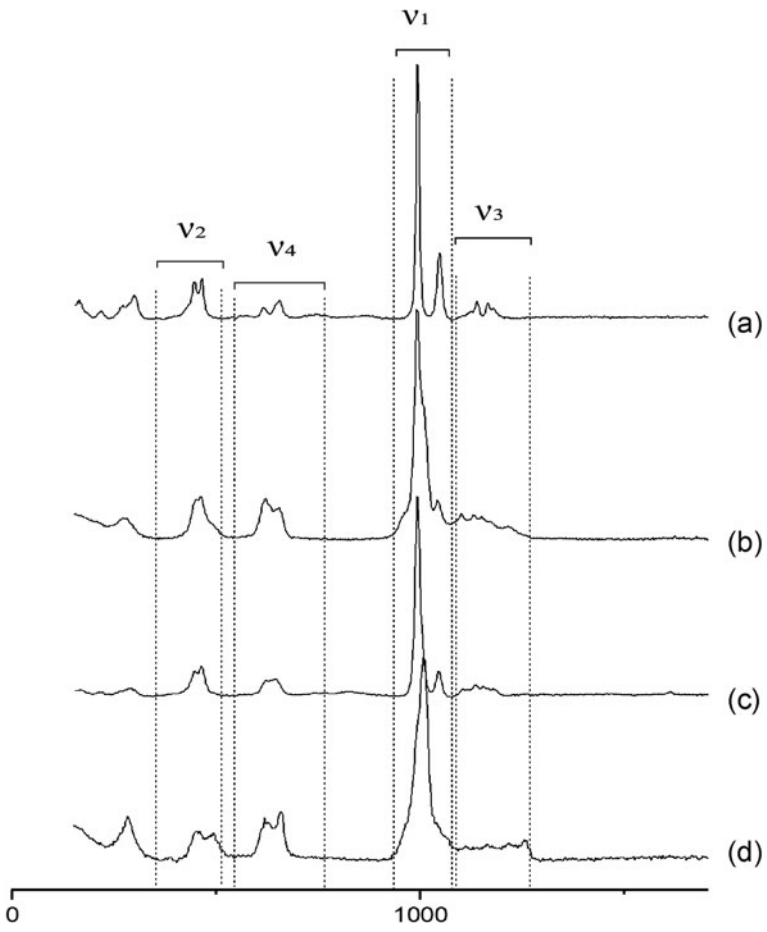

Figure 4. The Raman spectra of (a) saranchinaite, (b) petrovite, (c) dobrovolskyite and (d) cuprodobrovolskyite. For Raman shift values of bands see Table 2.

mode program in the range from 100 to 4000 cm^{-1} with the use of a holographic diffraction grating with 1800 lines/cm and a resolution of ~6 cm^{-1}. The diameter of the focal spot on the sample was ~10 μm. The Raman spectra were acquired on polycrystalline samples previously checked by powder X-ray diffraction (XRD).

Three main regions are usually distinguished in the Raman spectra of anhydrous sulfates with bivalent cations: (1) 800–1300 cm^{-1}, SO_4 stretching vibrations (ν_1 and ν_3 modes); (2) 800–400 cm^{-1}, SO_4 bending vibrations (ν_2 and ν_4 modes); (3) 400–100 cm^{-1}, *M*–O (*M* = Cu, Mg, Fe, Ca, Zn and Na) vibrations and lattice modes (Nakamoto, 1986; Kosek *et al.*, 2018 and references therein). Comparison of the Raman spectra of the above-listed minerals is presented in Fig. 4, Raman shift values and assignment of bands are given in Table 2.

Despite the common features, the Raman spectra of these sulfates are different from each other in numbers, intensities and positions of bands (Table 2). Symmetric bending vibrations of SO_4 tetrahedra in saranchinaite, petrovite and dobrovolskyite spectra appear in the range 447–464 cm^{-1}, whereas in cuprodobrovolskyite the positions of these bands are shifted to higher frequencies: 452–492 cm^{-1}. The band of asymmetric stretching vibrations of SO_4 tetrahedra in cuprodobrovolskyite has the highest frequency among these minerals: 1258 cm^{-1} (Table 2). Another distinctive feature of the spectrum of cuprodobrovolskyite is a single strong band at 1009 cm^{-1} (S–O stretching symmetric vibrations)

Table 2. Vibration modes of SO_4 tetrahedra in the Raman spectra of saranchinaite, petrovite, dobrovolskyite and cuprodobrovolskyite.

Mineral	Crystal system, space group	No.*	ν_2 – symmetric bending vibrations (350–500 cm^{-1})	ν_4 – asymmetric bending vibrations (600–800 cm^{-1})	ν_1 – symmetric stretching vibrations (950–1100cm^{-1})	ν_3 – asymmetric stretching (1100–1280 cm^{-1})
Saranchinaite	Monoclinic, $P2_1$	8	431sh, **447**, **464**	616, 619w, 628w, 644sh, 650sh, **654**	**993**, **1047**	**1139**, **1165**, 1179w
Petrovite	Monoclinic, $P2_1/c$	4	**451**, **462**, 493sh	621, 632sh, 647w, **654**	959sh, **991**, 1007sh, **1042**	**1100**, **1130**, **1150**, 1172, **1213**
Dobrovolskyite	Trigonal, *R*3	6	421, **447**, **464**	**620**, **631**, **643**,	992, 1045	**1104**, 1114, **1135**, **1154**, **1178**
Cuprodobrovolskyite	Trigonal, *R*3	6	**452**, 455sh, 462sh, 480sh, **492**	611sh, **618**, 628w, 647w, **657**	993sh, **1009**, 1044sh, 1064w	**1114**, **1163**, **1216**, **1258**, 1273

* 'No.' = Number of non-equivalent S sites (per unit cell)
Notes: sh – shoulder, w – weak band; strong bands are highlighted in bold type, bands with medium intensity have no marks.

https://doi.org/10.1180/mgm.2023.85 Published online by Cambridge University Press

Table 3. Powder X-ray diffraction data (d in Å) for cuprodobrovolskyite.

I_{meas}	d_{meas}	I_{calc}	d_{calc}	$h\ k\ l$	I_{meas}	d_{meas}	I_{calc}	d_{calc}	$h\ k\ l$	I_{meas}	d_{meas}	I_{calc}	d_{calc}	$h\ k\ l$
38	**11.66**	50	11.569	1 0 1	6	2.744	2	2.751	4 1 $\bar{3}$	1	1.958	1	1.962	4 4 0
		51	11.569	1 $\bar{1}$ $\bar{1}$			2	2.751	4 1 3			1	1.962	8 $\bar{4}$ 0
*33	7.28	1	7.339	0 0 $\bar{3}$			2	2.751	5 $\bar{4}$ 3	26	1.927	10	1.929	5 1 7
		1	7.339	0 0 3	6	2.731	2	2.714	3 2 4			1	1.929	6 $\bar{1}$ 7
4	6.51	6	6.496	2 $\bar{2}$ 1			2	2.714	5 $\bar{2}$ 4			17	1.928	6 0 6
		6	6.496	2 0 $\bar{1}$	6	2.692	1	2.699	5 0 $\bar{1}$			11	1.928	6 $\bar{6}$ 6
18	5.80	19	5.784	2 0 2			1	2.697	1 $\bar{1}$ 8			3	1.920	2 0 11
		20	5.784	2 $\bar{2}$ $\bar{2}$			1	2.697	1 0 $\bar{8}$	2	1.901	1	1.901	4 $\bar{3}$ 10
1	5.37	2	5.361	1 1 3	**68**	**2.615**	91	2.617	6 $\bar{3}$ 0	3	1.885	2	1.887	4 $\bar{5}$ 9
		4	5.361	2 $\bar{1}$ 3			92	2.617	3 3 0			2	1.887	5 $\bar{1}$ $\bar{9}$
4	5.12	6	5.102	1 0 4	*10	2.554	2	2.552	4 $\bar{6}$ 1	5	1.874	1	1.876	6 1 5
6	5.01	5	5.005	2 1 1			1	2.551	2 0 8			2	1.872	5 2 $\bar{6}$
		3	5.005	3 $\bar{1}$ 1	1	2.502	2	2.502	4 2 2			1	1.872	7 $\bar{2}$ 6
22	4.665	14	4.657	3 $\bar{2}$ 2	1	2.466	1	2.464	3 3 3			2	1.872	7 $\bar{5}$ 6
		20	4.657	2 $\bar{3}$ 2	7	2.422	1	2.427	6 $\bar{1}$ 1	4	1.832	5	1.834	0 0 $\bar{12}$
		13	4.657	2 1 $\bar{2}$	1	2.387	1	2.384	5 $\bar{6}$ 2			5	1.834	0 0 12
19	4.536	26	4.532	3 0 0	5	2.329	2	2.328	4 2 $\bar{4}$	4	1.822	2	1.822	4 3 7
		26	4.532	3 $\bar{3}$ 0			2	2.328	6 $\bar{4}$ 4			3	1.822	7 $\bar{3}$ 7
2	4.274	2	4.278	2 $\bar{2}$ 4	3	2.310	2	2.313	5 0 5	2	1.800	2	1.801	7 1 0
		3	4.278	2 0 $\bar{4}$	7	2.265	8	2.266	6 0 0			2	1.801	8 $\bar{7}$ 0
1	4.204	2	4.189	1 0 $\bar{5}$			9	2.266	6 $\bar{6}$ 0	2	1.778	1	1.777	5 3 5
		3	4.189	1 $\bar{1}$ 5	11	2.222	4	2.224	4 3 1			3	1.777	7 0 $\bar{5}$
100	**3.859**	71	3.856	3 0 3			3	2.224	7 $\bar{3}$ 1			1	1.777	8 $\bar{3}$ 5
		100	3.856	3 $\bar{3}$ 3	4	2.186	2	2.177	5 2 0			2	1.777	7 $\bar{7}$ 5
		99	3.856	3 0 $\bar{3}$			1	2.177	7 $\bar{2}$ 0	1	1.747	2	1.749	8 $\bar{1}$ 3
36	**3.702**	23	3.717	3 1 $\bar{1}$			2	2.177	7 $\bar{5}$ 0			1	1.749	7 1 3
		4	3.717	3 $\bar{4}$ 1			1	2.177	5 $\bar{7}$ 0	3	1.731	2	1.735	4 3 $\bar{8}$
		23	3.717	4 $\bar{3}$ 1	7	2.165	4	2.165	6 $\bar{6}$ 3			2	1.735	7 $\bar{4}$ 8
39	**3.674**	40	3.669	0 0 6			3	2.165	6 0 $\bar{3}$			1	1.733	6 2 $\bar{5}$
		39	3.669	0 0 $\bar{6}$	*5	2.130	1	2.139	4 $\bar{4}$ 8	2	1.712	1	1.719	5 4 $\bar{2}$
8	3.569	6	3.567	3 1 2			1	2.139	4 0 $\bar{8}$			1	1.719	9 $\bar{5}$ 2
		5	3.567	4 $\bar{1}$ 2	4	2.086	1	2.087	7 $\bar{5}$ 3	3	1.693	4	1.694	8 0 $\bar{1}$
2	3.462	4	3.461	4 $\bar{2}$ 3			1	2.087	5 2 $\bar{3}$			4	1.694	8 $\bar{8}$ 1
		5	3.461	2 2 $\bar{3}$			2.	2.087	5 $\bar{7}$ 3	*4	1.679	1	1.679	8 0 2
		3	3.461	2 2 3	4	2.075	1	2.076	2 2 9	4	1.651	3	1.652	5 3 $\bar{7}$
3	3.343	3	3.359	4 $\bar{4}$.$\bar{1}$			2	2.076	4 $\bar{2}$ 9			3	1.652	8 $\bar{5}$ 7
		3	3.359	4 0 1			2	2.076	2 2 $\bar{9}$	1	1.623	1	1.626	5 $\bar{7}$ 9
8	3.250	13	3.248	4 $\bar{4}$ 2			1	2.071	4 3 4	2	1.615	1	1.616	7 1 6
		13	3.248	4 0 $\bar{2}$	3	2.060	1	2.063	3 2 $\bar{8}$	2	1.585	1	1.587	8 1 1
46	**3.086**	21	3.088	3 2 1			1	2.063	5 $\bar{3}$ 8	2	1.578	2	1.575	8 $\bar{9}$ 2
		36	3.088	5 $\bar{2}$ 1	4	1.988	5	1.990	4 $\bar{6}$ 7	1	1.568	1	1.568	4 3 10
12	2.973	7	2.967	4 1 0			2	1.990	6 $\bar{4}$ 7	4	1.550	1	1.555	6 4 $\bar{1}$
		4	2.967	5 $\bar{1}$ 0			3	1.990	4 2 $\bar{7}$			1	1.555	10 $\bar{6}$ 1
		3	2.967	4 $\bar{5}$ 0	3	1.980	1	1.980	1 $\bar{1}$ $\bar{11}$			2	1.552	9 $\bar{3}$ 6
		7	2.967	5 $\bar{4}$ 0			1	1.980	1 0 $\bar{11}$			2	1.552	6 $\bar{9}$ 6
6	2.912	3	2.892	4 0 4						4	1.509	5	1.510	9 0 0
*99	**2.853**	22	2.854	2 $\bar{2}$ 7								5	1.510	9 $\bar{9}$ 0
		22	2.854	2 0 $\bar{7}$						3	1.502	2	1.502	3 3 $\bar{12}$
		60	2.852	3 0 $\bar{6}$								2	1.502	3 3 12
		46	2.852	3 0 6								2	1.502	6 $\bar{3}$ 12
		47	2.852	3 $\bar{3}$ $\bar{6}$										
		59	2.852	3 $\bar{3}$ 6										

*Reflections overlapped with reflections of admixed petrovite. The strongest reflections are marked in boldtype.

with shoulders (1044 and 1064 cm^{-1}), whereas in the spectra of saranchinaite, petrovite and dobrovolskyite there are distinct doublets: strong band at 991–993 cm^{-1} and weaker band at 1042–1047 cm^{-1}.

The absence of bands with frequencies higher than 1300 cm^{-1} indicates the absence of groups with O–H, C–H, C–O, N–H and N–O bonds in cuprodobrovolskyite and other studied sulfates.

Powder X-ray diffraction data and crystal structure

The attempts of single-crystal XRD studies of cuprodobrovolskyite were unsuccessful because of the imperfectness (microblocky character) of crystals. Powder XRD data for the new mineral (on a sample polluted with petrovite and saranchinaite) were collected using a Rigaku R-AXIS Rapid II diffractometer equipped with image plate detector and rotating anode with the microfocus optics, Co$K\alpha$ radiation, 40 kV, 15 mA, Debye-Scherrer geometry, d = 127.4 mm and exposure time of 15 min. The raw data to profile conversion was performed with the *osc2xrd* program (Britvin *et al.*, 2017). Powder data are reported in Table 3. On the basis of the data on dobrovolskyite (Shablinskii *et al.*, 2021), we found that the mineral is trigonal, space group $R3$. The unit-cell parameters of cuprodobrovolskyite calculated from the powder data are: a = 15.702(2), c = 22.017(5) Å, V = 4701.0(2) Å^3, and Z = 9.

https://doi.org/10.1180/mgm.2023.85 Published online by Cambridge University Press

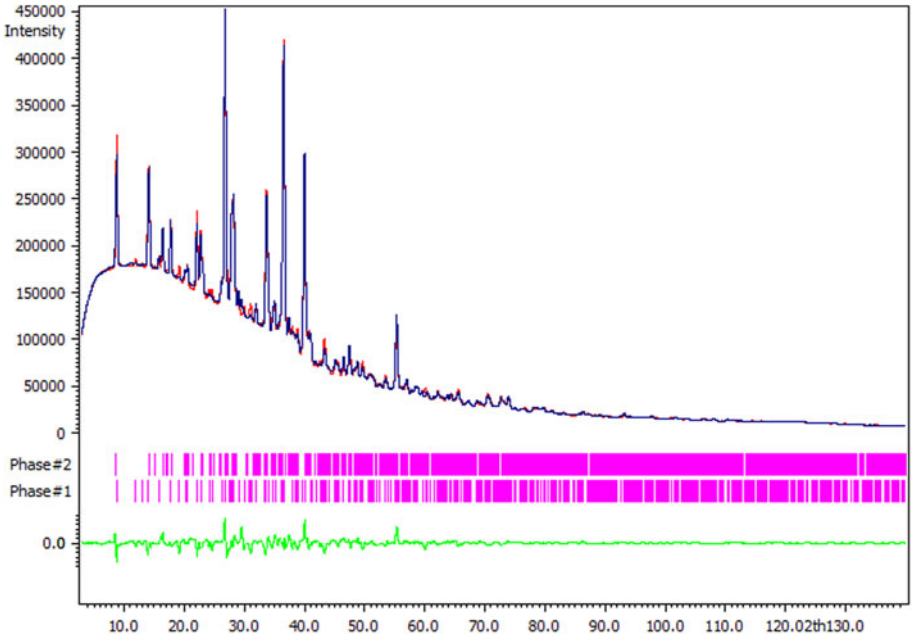

Figure 5. Rietveld refinement plot of mixture of cuprodobrovolskyite and petrovite. The models of dobrovolskyite (Shablinskii *et al.*, 2021) (Phase #1; see Table 4) and petrovite (Filatov *et al.*, 2020) (Phase #2) were used, Bragg positions of their reflections are coloured in magenta. The blue curve is the experimental pattern of the mixture consisting of cuprodobrovolskyite and petrovite, the calculated pattern is outlined in red, the difference curve is outlined in green.

Table 4. Comparative data on cuprodobrovolskyite and related minerals.

Mineral	Cuprodobrovolskyite*	Dobrovolskyite	Petrovite	Saranchinaite	Bubnovaite
Ideal formula	$Na_4Cu(SO_4)_3$	$Na_4Ca(SO_4)_3$	$Na_{12}Cu_2(SO_4)_8$	$Na_2Cu(SO_4)_2$	$K_2Na_8Ca(SO_4)_6$
Crystal system	Trigonal	Trigonal	Monoclinic	Monoclinic	Trigonal
Space group	*R*3	*R*3	$P2_1/c$	$P2_1$	*P*31*c*
a (Å)	15.702(2)	15.7223(2)	12.615(2)	9.0109(5)	10.804(3)
b (Å)			9.026(1)	15.6355(8)	
c (Å)	22.017(2)	22.0160(5)	12.717(2)	10.1507(5)	22.011(6)
β (°)			108.311(3)	107.079(2)	
V (Å^3)	4701.0(2)	4713.1(2)	1374.7(3)	1367.06(12)	2225(1)
Z	18	18	2	8	4
Strongest reflections of the measured powder X-ray diffraction pattern: *d*, Å – *I*	11.56–50 5.78–20 3.85–100 3.72–23 3.66–40 3.08–36 2.852–60 2.617–92	11.58–40 5.79–22 3.86–88 3.67–32 3.11–24 3.09–26 2.855–50 2.682–100	7.24–100 7.21–27 6.25–38 4.47–31 3.95–21 3.70–36 3.65–34 2.60–48 2.57–37	8.61–42 7.82–59 7.67–47 6.09–49 4.63–46 3.76–100 2.71–98 2.53–64	3.943–80 2.894–35 2.868–62 2.718–91 2.707–100 2.647–10 2.231–60 1.969–21
Optical data	Uniaxial (+) ω = 1.509(3) ε = 1.528(3)	Uniaxial (+) ω = 1.489(2) ε = 1.491(2)	Biaxial (+) α = 1.498(3) β = 1.500 γ = 1.516(3)	Biaxial (+) α = 1.517(2) β = 1.531(2) γ = 1.559(2)	Uniaxial (–) ω = 1.492(2) ε = 1.489(2)
Reference	This study	Shablinskii *et al.* (2021)	Filatov *et al.* (2020)	Siidra *et al.* (2018)	Gorelova *et al.* (2016)

*The formula of cuprodobrovolskyite is given for *Z* = 18 for better comparison with other presented minerals.

The crystal structure of cuprodobrovolskyite was studied on a powder sample using the Rietveld method. Data treatment and the Rietveld structure analysis were carried out using the *Jana2006* software (Petříček *et al.*, 2014). A total of 13,700 observed intensity envelope points were used in the refinement. The profiles of individual reflections were modelled using a Pseudo-Voigt function.

The refinement of the crystal structure of cuprodobrovolskyite was complicated by the presence of admixed petrovite and saranchinaite in the powder sample (Fig. 5). As shown in Table 4, cuprodobrovolskyite is well-distinguished from petrovite and saranchinaite by number and position of strong reflections in powder XRD pattern. Generally, the powder XRD diagram is a good diagnostic tool to distinguish cuprodobrovolskyite from other Na–Cu sulfates including petrovite though quite similar in chemistry.

Data collection information and structure refinement details for cuprodobrovolskyite are given in Table 5. However, the pollution of the sample by these two minerals led to the insufficient description of the profile, which affected the refinement of anisotropic displacement parameters for O atoms and metals. The accuracy of calculations of the location of O atoms and, respectively, the interatomic *M*–O and *S*–O distances did not allow us to calculate the BVS. Atomic scattering factors together with

https://doi.org/10.1180/mgm.2023.85 Published online by Cambridge University Press

Table 5. Crystal data and Rietveld refinement details for cuprodobrovolskyite.

Formula (from structure refinement)	$(Na_{7.21}\square_{0.79})(Cu_{1.23}Ca_{0.77})(SO_4)_6$
Crystal system	Trigonal
Space group	*R*3
a (Å)	15.702 (2)
c (Å)	22.017(5)
V (Å^3)	4701.0(2)
Z	9
Radiation; wavelength (Å)	Co*Kα*; 1.79021
Temperature (K)	293
F(000)	1139
2θ range for data (°)	3.00 to 139.99
Profile function	Pseudo-Voight
Background function	36 Legendre polynomial
Final *R* indices	$R_p = 0.0246$, $R_{wp} = 0.0325$ $R_1 = 0.0521$, $wR_2 = 0.0770$

Table 6. Coordinates and equivalent displacement parameters (Å^2) of atoms and site occupancies in crystal structure of cuprodobrovolskyite.

Site	*x/a*	*y/b*	*z/c*	U_{eq}	Site occupancy
*M*1	0	0	0.749(2)	0.064(3)	Na
*M*2	0	0	0.382(1)	0.055(5)	Na
*M*3	0.523(1)	0.416(2)	0.504(1)	0.112(2)	Na
*M*4	0.909(2)	0.792(1)	0.481(2)	0.038(6)	Na
*M*5	0	0	0.574(1)	0.071(3)	Na
*M*6	0.661(1)	0.725(1)	0.574(2)	0.071(4)	Na
*M*7	0.664(2)	0.979(1)	0.576(2)	0.007(1)	$Na_{0.88(2)}\square_{0.12}$
*M*8	0	0	0.233(2)	0.056(4)	$Na_{0.79(2)}\square_{0.21}$
*M*9	0.451(2)	0.892(1)	0.658(1)	0.029(3)	$Na_{0.94(2)}\square_{0.06}$
*M*10	⅔	⅓	0.407(1)	0.035(4)	Na
*M*11	0.697(2)	0.984(1)	0.719(1)	0.042(2)	Na
*M*12	⅓	⅔	0.559(2)	0.064(4)	$Na_{0.60(2)}\square_{0.40}$
*M*13	0.130(2)	0.880(1)	0.310(1)	0.018(3)	$Cu_{0.70(2)}Ca_{0.30}$
*M*14	0.705(1)	0.711(2)	0.738(1)	0.056(3)	$Cu_{0.53(2)}Ca_{0.47}$
S1	0.903(1)	0.802(1)	0.629(1)	0.030(2)	S
S2	0.113(2)	0.888(1)	0.475(2)	0.050(7)	S
S3	0.570(1)	0.108(2)	0.661(1)	0.024(3)	S
S4	0.766(1)	0.559(1)	0.488(2)	0.051(2)	S
S5	0.437(2)	0.555(1)	0.512(1)	0.052(5)	S
S6	0.556(1)	0.777(2)	0.687(1)	0.025(6)	S
O1	0.906(1)	0.832(1)	0.570(1)	0.04(1)	O
O2	0.547(2)	0.607(1)	0.524(1)	0.09(3)	O
O3	0.160(1)	0.870(1)	0.414(2)	0.10(2)	O
O4	0.796(2)	0.727(2)	0.630(1)	0.06(1)	O
O5	0.092(1)	0.965(1)	0.486(1)	0.09(2)	O
O6	0.925(1)	0.857(1)	0.688(1)	0.07(3)	O
O7	0.752(1)	0.464(2)	0.466(1)	0.10(1)	O
O8	0.216(1)	0.961(1)	0.480(2)	0.12(3)	O
O9	0.437(1)	0.618(2)	0.568(1)	0.08(2)	O
O10	0.613(1)	0.736(1)	0.655(1)	0.08(1)	O
O11	0.384(1)	0.447(1)	0.512(1)	0.12(3)	O
O12	0.946(1)	0.746(1)	0.647(1)	0.03(2)	O
O13	0.720(1)	0.585(1)	0.537(1)	0.13(4)	O
O14	0.526(2)	0.022(1)	0.708(1)	0.09(2)	$O_{0.5}$
O15	0.522(1)	0.169(2)	0.692(1)	0.06(2)	$O_{0.5}$
O16	0.593(1)	0.874(1)	0.659(2)	0.07(1)	O
O17	0.397(1)	0.594(1)	0.464(1)	0.07(1)	O
O18	0.608(2)	0.824(1)	0.744(1)	0.12(3)	O
O19	0.659(1)	0.210(2)	0.659(1)	0.12(6)	O
O20	0.450(2)	0.706(1)	0.690(1)	0.13(3)	O
O21	0.069(2)	0.777(1)	0.471(1)	0.10(4)	$O_{0.5}$
O22	0.776(2)	0.638(2)	0.448(1)	0.14(5)	O
O23	0.875(1)	0.610(1)	0.505(1)	0.07(3)	O
O24	0.152(1)	0.895(1)	0.532(2)	0.10(2)	$O_{0.5}$
O25	0.550(2)	0.135(1)	0.598(1)	0.16(5)	O
O26	0.622(1)	0.050(1)	0.640(2)	0.11(3)	$O_{0.5}$
O27	0.621(1)	0.122(2)	0.720(1)	0.11(4)	$O_{0.5}$

anomalous dispersion corrections were taken from the *International Tables for X-Ray Crystallography* (Ibers and Hamilton, 1974). The final refinement cycles were finished with $R_p = 0.0246$, $R_{wp} = 0.0325$, $R_1 = 0.0521$, $wR_2 = 0.0770$ and GOF = 7.70 for all data. Fractional atomic coordinates, site occupancies based on refined electron numbers and equivalent atomic displacement parameters (U_{eq}) are given in Table 6. The selected interatomic distances in the cuprodobrovolskyite structure are presented in Table 7. The crystallographic information file has been deposited with the Principal Editor of *Mineralogical Magazine* and is available as Supplementary material (see below). All SO_4 tetrahedra are quite distorted with S–O distances from 1.37 to 1.62 Å. For two S sites (S2 and S3), coordination of S by O atoms includes additional variative O sites by analogy with dobrovolskyite. Sodium atoms centre different polyhedra, with coordination numbers from 6 to 9 (Table 7). These polyhedra, joining *via* edges, vertices and SO_4 tetrahedra, form rods described by Shablinskii *et al.* (2021) for dobrovolskyite. Cu^{2+} cations occupy two independent *M* sites coordinated by seven O atoms with average distances of 2.39 and 2.66 Å for *M*13 and *M*14, respectively. The refined numbers of electrons (e_{ref}) are 26 for *M*13 and 25 for *M*14 whereas for other cation sites e_{ref} were between 6 and 12. The only 'heavy' component, which is present in the mineral in a significant amount to cause e_{ref} values for *M*13 = 26 and for *M*14 = 25, is Cu, whereas the amounts of other constituents with high atomic numbers, Pb and Zn, are minor: 0.04 and 0.07 apfu, respectively. Thus, it is undoubtedly Cu that is the prevailing cation in both *M*13 and *M*14 sites. The second component in *M*13 and *M*14 should be Ca. This consideration is supported by two arguments: (1) in the isostructural mineral dobrovolskyite, ideally $Na_4Ca(SO_4)_3$, Ca occurs in these sites (Shablinskii *et al.*, 2021); and (2) in synthetic analogue of the Cu-bearing variety of dobrovolskyite, $Na_4(Ca,Cu)(SO_4)_3$, both Ca and Cu^{2+} occupy these sites together (Shorets, 2022).

Heat treatment of cuprodobrovolskyite

The heating of greenish-blue crusts composed of cuprodobrovolskyite with ingrowths of petrovite and saranchinaite at 600°C for 4 h was carried out using the muffle furnace. The experiment reveals that only cuprodobrovolskyite remains in the sample (verified by powder XRD: Fig. 6). The colour of the sample changed after heating from blue to light green. The chemical composition of the obtained crystals is close to that of cuprodobrovolskyite before the heating (Table 1). Notably, the studied mixture partly decomposed with segregation of CuO on the crucible walls.

Discussion

Comparative crystal chemistry of anhydrous sodium–copper sulfates

Three natural anhydrous Na–Cu sulfates without additional oxygen, saranchinaite $Na_2Cu(SO_4)_2$, petrovite $Na_{12}Cu_2(SO_4)_8$, and cuprodobrovolskyite $Na_4Cu(SO_4)_3$ belong to three different structural types. The main structural units in these minerals are based on motifs built by Cu^{2+}-centred polyhedra and SO_4 tetrahedra, however, there are significant differences (Fig. 7). Saranchinaite is considered as a specific compound with a three-dimensional $[Cu_4(SO_4)_8]^{8-}$ framework (Siidra *et al.*, 2017) whereas the crystal structure of petrovite includes isolated $[Cu_2(SO_4)_8]^{12-}$ clusters in which CuO_7 polyhedra are connected *via* vertices with SO_4

https://doi.org/10.1180/mgm.2023.85 Published online by Cambridge University Press

Table 7. Selected interatomic distances in crystal structure of cuprodobrovolskyite.

*M*1 (Na)	–O17	2.13(2) ×3	*M*9 (Na)	–O14	2.08(2)	S1	–O12	1.41(2)
	–O6	2.36(2) ×3		–O9	2.27(2)		–O6	1.50(2)
*M*2 (Na)	–O19	2.25(2) ×3		–O16	2.38(2)		–O4	1.49(2)
	–O15	2.49(2) ×3		–O20	2.50(2)		–O1	1.37(2)
	–O5	2.90(2) ×3		–O26	2.62(2)	S2	–O3	1.62(2)
*M*3 (Na)	–O18	2.16(2)		–O10	2.83(2)		–O8	1.44(2)
	–O25	2.23(2)	*M*10 (Na)	–O20	1.96(2) ×3		–O5	1.42(2)
	–O23	2.24(2)		–O7	2.23(2) ×3		–O21	1.52(2)
	–O7	2.27(2)	*M*11 (Na)	–O12	2.14(2)		–O24	1.38(2)
	–O11	2.46(2)		–O16	2.14(2)	S3	–O27	1.48(2)
	–O2	2.86(2)		–O18	2.24(2)		–O19	1.50(2)
*M*4 (Na)	–O1	2.06(2)		–O21	2.57(2)		–O25	1.52(2)
	–O5	2.16(2)		–O26	2.59(2)		–O14	1.56(2)
	–O27	2.20(2)		–O6	2.66(2)		–O26	1.56(2)
	–O22	2.38(2)		–O11	2.93(2)		–O15	1.61(2)
	–O8	2.51(2)		–O27	2.95(2)	S4	–O22	1.46(2)
	–O21	2.64(2)	*M*12 (Na)	–O9	2.12(2) ×3		–O13	1.46(2)
	–O23	2.68(2)		–O17	2.79(2) ×3		–O7	1.48(2)
	–O14	2.73(2)	*M*13 ($Cu_{0.70}Ca_{0.30}$)	–O19	2.16(2)		–O23	1.52(2)
*M*5 (Na)	–O1	2.29(2) ×3		–O4	2.21(2)	S5	–O11	1.47(2)
	–O5	2.63(2) ×3		–O15	2.25(2)		–O17	1.51(2)
*M*6 (Na)	–O24	1.93(2)		–O3	2.36(2)		–O2	1.51(2)
	–O10	1.98(2)		–O12	2.53(2)		–O9	1.58(2)
	–O2	2.12(2)		–O13	2.57(2)	S6	–O20	1.47(2)
	–O8	2.37(2)		–O26	2.66(2)		–O16	1.46(2)
	–O4	2.43(2)	*M*14 ($Cu_{0.53}Ca_{0.47}$)	–O3	2.45(2)		–O18	1.48(2)
	–O13	2.89(2)		–O10	2.48(2)		–O10	1.51(2)
*M*7 (Na)	–O11	2.08(2)		–O8	2.55(2)			
	–O26	2.10(2)		–O4	2.72(2)			
	–O16	2.33(2)		–O22	2.78(2)			
	–O12	2.42(2)		–O2	2.83(2)			
	–O23	2.52(2)		–O18	2.86(2)			
	–O21	2.63(2)						
*M*8 (Na)	–O19	2.77(2) ×3						
	–O25	2.79(2) ×3						
	–O7	2.85(2) ×3						

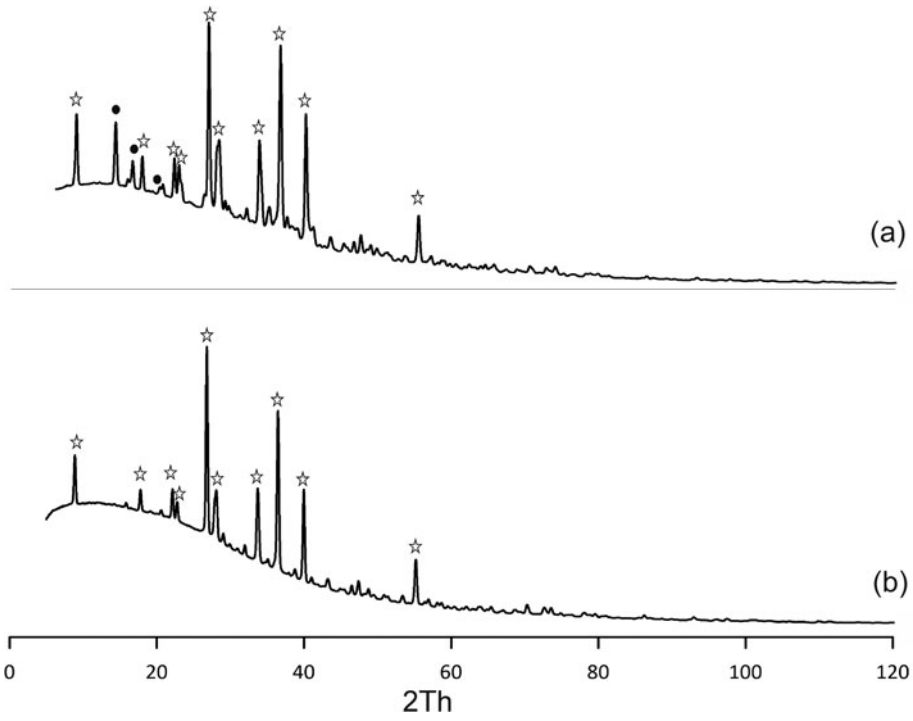

Figure 6. Powder X-ray diffraction patterns (λ = 1.79021 Å) of cuprodobrovolskyite with (a) a petrovite admixture and (b) the same sample after heating to 600°C for 4 hours in a muffle furnace. The distinctive reflections of cuprodobrovolskyite and petrovite are marked as stars and filled circles, respectively.

https://doi.org/10.1180/mgm.2023.85 Published online by Cambridge University Press

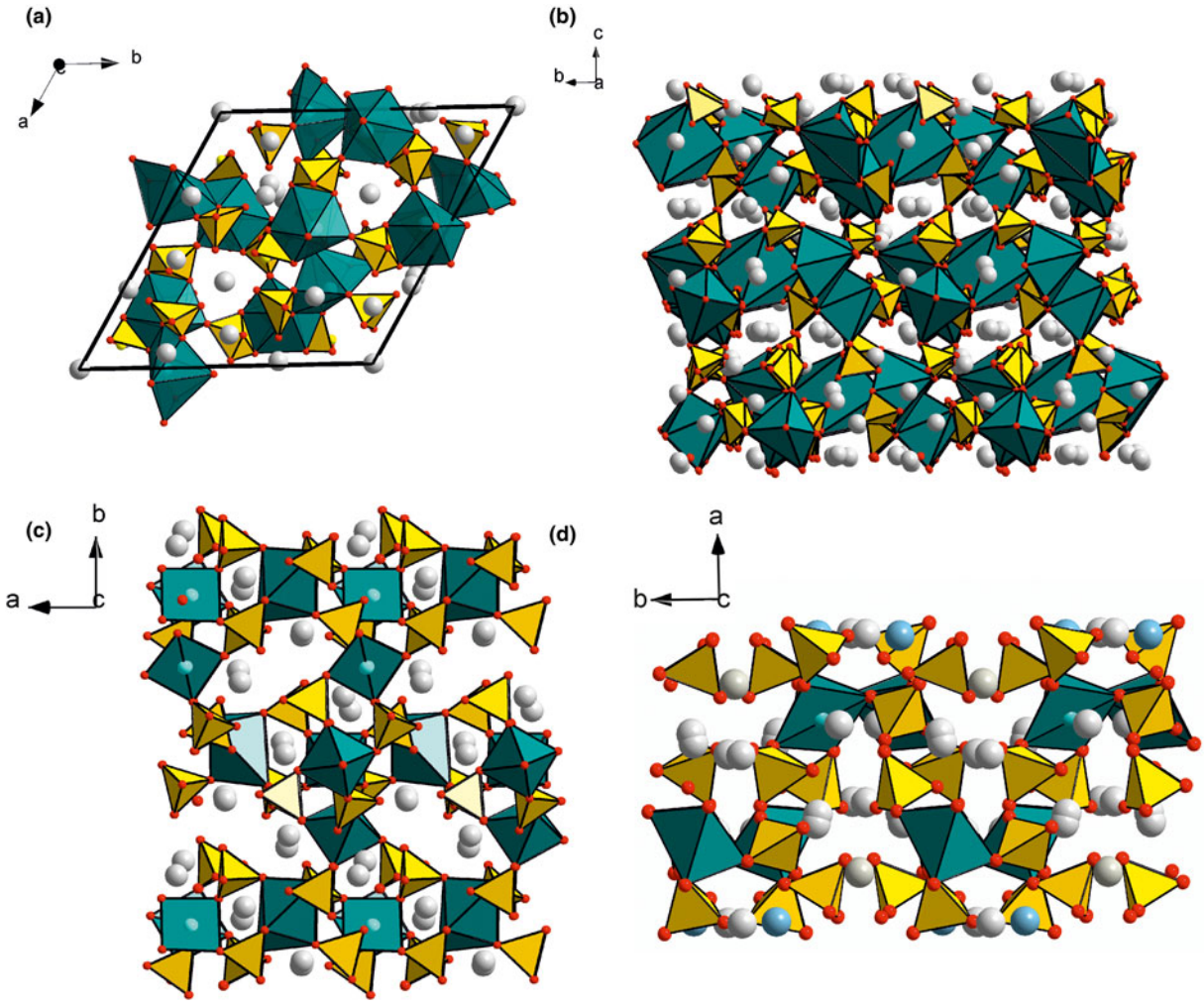

Figure 7. The fragments of crystal structures of (a and b) cuprodobrovolskyite, (c) saranchinaite (drawn after Siidra *et al.*, 2018) and (d) petrovite (drawn after Filatov *et al.*, 2020). SO_4 tetrahedra are yellow, Cu-centred polyhedra are bluish-green, Na atoms are presented as greyish spheres. Drawn using *Diamond 3.2* (Diamond - Crystal and Molecular Structure Visualization, Crystal Impact - Dr. H. Putz & Dr. K. Brandenburg GbR, Kreuzherrenstr. 102, 53227 Bonn, Germany, https://www.crystalimpact.de/diamond).

tetrahedra (Filatov *et al.*, 2020). In all three discussed crystal structures, Cu^{2+} cations centre 7-fold polyhedra (in saranchinaite there are also CuO_6 octahedra with Jahn–Teller distortion). In cuprodobrovolskyite, Cu-centred 7-fold polyhedra are linked to each other *via* common edges, the same as Ca polyhedra in dobrovolskyite (Fig. 8). The joint of SO_4 tetrahedra with CuO_7 polyhedra in cuprodobrovolskyite is illustrated in Fig. 9.

It is noteworthy that the crystal structures with edge-shared Cu-polyhedra are not exotic. There are numerous compounds with such type of Cu polyhedra stacking, e.g. walls composed of CuO_5 polyhedra are described for α-$(Cu_{2-x}Zn_x)V_2O_7$ (Shi *et al.*, 2020) and chains of edge-shared CuO_6 octahedra for β-$NaCuPO_4$ (Ulutagay-Kartin *et al.*, 2002). The experiments performed by Siidra *et al.* (2021) clearly show that the appearance of highly-coordinated Cu^{2+} (7-fold coordination by O atoms) is, in general, not unique for anhydrous alkali copper sulfates. Cuprodobrovolskyite is one more example which demonstrates this phenomenon.

Cuprodobrovolskyite belongs to the family of sulfates with structures derived from the archetype of hexagonal (space group $P6_3/mmc$) sodium sulfate with an aphthitalite-like structure known among synthetic compounds as Na_2SO_4(I) (Fischmeister, 1962; Rasmussen *et al.*, 1996 and references therein) and in Nature as metathénardite (Pekov *et al.*, 2019). Its trigonal derivatives with the same unit-cell metrics ($a = 5.3$–5.8 and $c = 7.05$–7.4 Å) are aphthitalite $K_3Na(SO_4)_2$, natroaphthitalite $KNa_3(SO_4)_2$ (both $P\bar{3}m1$), and belomarinaite $KNaSO_4$ ($P3m1$) (Filatov *et al.*, 2019; Shchipalkina *et al.*, 2020a). The derivatives with multiplied unit-cell parameters are bubnovaite $K_2Na_8Ca(SO_4)_6$, ($P31c$, $a = 10.8$ and $c = 22.0$ Å, Gorelova *et al.*, 2016), dobrovolskyite $Na_4Ca(SO_4)_3$ (Shablinskii *et al.*, 2021), and cuprodobrovolskyite $Na_4Cu(SO_4)_3$ (both $R3$, $a = 15.7$ and $c = 22.0$ Å: Table 4). All these minerals, except for aphthitalite, were described as new species in exhalations of the Tolbachik fumaroles. The relationship of the dobrovolskyite structure type with the archetype of metathénardite and relative superstructures such as bubnovaite $K_2Na_8Ca(SO_4)_6$ and hanksite $Na_{22}K(SO_4)_9(CO_3)_2Cl$ was described by Shablinskii *et al.* (2021). They represented the series of aphthitalite-related crystal structures in terms of stacking cation layers and their arrangement in unit cells. The dobrovolskyite structure is considered as unique with a 3×3×3 superstructure and ordered vacant sites in the cation array (Shablinskii *et al.*, 2021). It is interesting that the dobrovolskyite structure type is suitable for isomorphism of $Cu^{2+} \rightarrow Ca$ despite the discrepancy

https://doi.org/10.1180/mgm.2023.85 Published online by Cambridge University Press

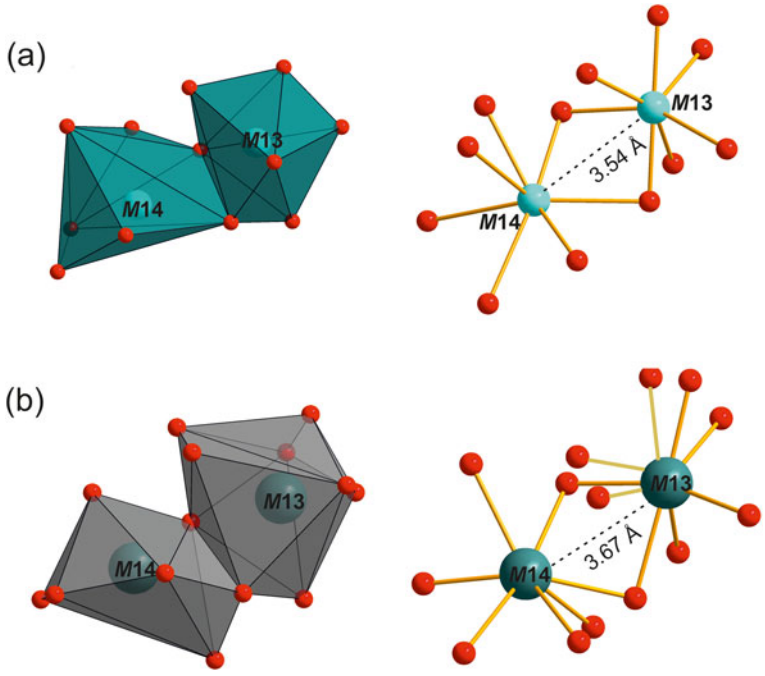

Figure 8. Coordination of Cu and Ca atoms and joint of Cu- and Ca-centred polyhedra (*M*13 and *M*14) in crystal structures of (a) cuprodobrovolskyite and (b) dobrovolskyite (drawn after Shablinskii *et al.*, 2021).

in their ionic radii: 0.72 and 1.06 Å for Cu^{2+} and Ca, respectively (Shannon and Prewitt, 1969). However, there are several proved examples of solid-solution series between isotypic Ca- and Cu-compounds. The crystal structure data on these compounds show that positions of Ca^{2+} and Cu^{2+} cations are not exactly the same though they are located closely. Thus, among relatively simple compounds, the synthetic solid-solution series $Ca_{1-x}Cu_{2+x}O_3$ is a promising example (Ruck *et al.*, 2001). In Nature for example, alluaudite-group minerals show such a phenomenon. The most demonstrative example here is the continuous solid-solution series johillerite $NaCuMg_3(AsO_4)_3$ – nickenichite $Na(Ca_{0.5}Cu_{0.5})Mg_3(AsO_4)_3$ – calciojohillerite $NaCaMg_3(AsO_4)_3$: in intermediate members, the closely located *A*(1) and *A*(1)' sites are occupied with Ca and Cu^{2+}, respectively [Hatert, 2019, and references therein). Another interesting example of isomorphous substitution of Ca by Cu was stated for synthetic hydroxylapatite (Guo *et al.* 2021). According to the crystal chemical data obtained in this work, a similar character of Ca–Cu^{2+} substitution in cuprodobrovolskyite and dobrovolskyite can be proposed, especially noting the unusual interatomic distances for Ca and Cu. Thus, these cations can occupy the closely located positions. The relatively high values of atom displacement parameters for the cation sites, especially *M*14 (Table 6), as well as significant distortion of polyhedra, could be a result of a splitting of the *M*13 and *M*14 sites to subsites statistically occupied with Cu or Ca. It is not excluded that these subsites could be described with different oxygen coordinations, however, the quality of the available samples does not allow us to prove this suggestion. It is noteworthy, that the recently IMA-approved mineral enricofrancoite (IMA No. 2023-002) with the ideal formula $KNaCaSi_4O_{10}$ from the Somma-Vesuvius volcanic complex (Naples, Italy) is an analogue of litidionite $KNaCuSi_4O_{10}$ with Ca instead of Cu (Balassone *et al.*, 2023). This find is more indirect evidence that post-volcanic processes can contribute to Ca–Cu^{2+} isomorphic substitution.

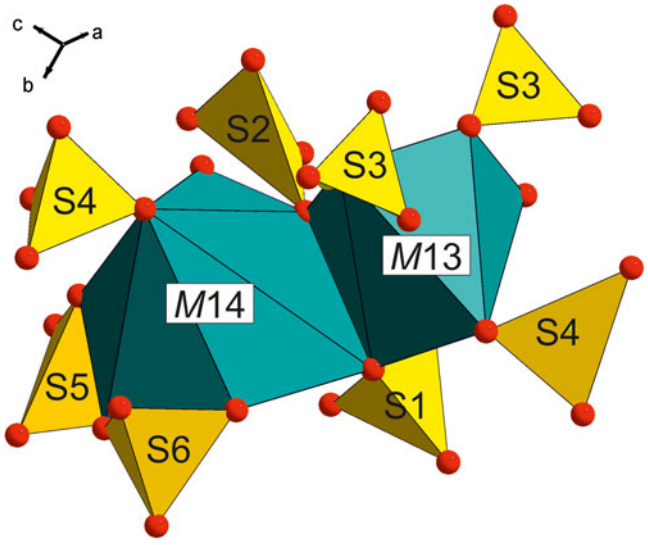

Figure 9. The fragment of the crystal structure of cuprodobrovolskyite with polyhedra centred by bivalent cations.

Genetic features of anhydrous Na–Cu sulfates: relationship between of saranchinaite $Na_2Cu(SO_4)_2$, petrovite $Na_{12}Cu_2(SO_4)_8$ and cuprodobrovolskyite $Na_4Cu(SO_4)_3$

As was shown by Siidra *et al.* (2018) for genesis of saranchinaite: (1) it can be a product of dehydration of kröhnkite $Na_2Cu(SO_4)_2(H_2O)_2$ with complete transformation at 200°C; and (2) at temperatures higher than 475°C saranchinaite decomposes into tenorite, thénardite (metathénardite? – *our note*) and an unidentified phase. The latter can correspond to petrovite or cuprodobrovolskyite, but the data given in the cited paper are scarce and do not allow comparison of the reflections on the powder XRD patterns.

If we assume that petrovite and cuprodobrovolskyite can be not only the primary sulfates but also the products of transformations of several associated minerals (of which there are many in

https://doi.org/10.1180/mgm.2023.85 Published online by Cambridge University Press

large amounts) in sulfate-rich zones of the Arsenatnaya fumarole, then the following reactions can be suggested:

$$Na_2Cu(SO_4)_2 \text{ (saranchinaite)} + Na_2SO_4 \text{ (metathénardite)} \rightarrow Na_4Cu(SO_4)_3 \text{ (cuprodobrovolskyite)},$$

$$Na_2Cu(SO_4)_2(H_2O)_2 \text{ (supergene kröhnkite)} + Na_2SO_4 \text{ (metathénardite)} \rightarrow Na_4Cu(SO_4)_3 \text{ (cuprodobrovolskyite)} + 2H_2O\uparrow,$$

$$2Na_4Cu(SO_4)_3 \text{ (cuprodobrovolskyite)} + 2Na_2SO_4 \text{ (metathénardite)} \rightarrow Na_{12}Cu_2(SO_4)_8 \text{ (petrovite)}.$$

Dobrovolskyite $Na_4Ca(SO_4)_3$ and cuprodobrovolskyite from the Arsenatnaya fumarole are supposed to form a solid-solution series, which is most probably, limited (Fig. 10). The presence of admixed Ca in both petrovite and the studied cuprodobrovolskyite could be due to the participation of anhydrite $CaSO_4$ in the reactions as suggested for petrovite by Filatov *et al.* (2020):

$$2Na_2Cu(SO_4)_2 \text{ (saranchinaite)} + CaSO_4 \text{ (anhydrite)} + 3Na_2SO_4 \text{ (metathénardite)} \rightarrow (Na_{10}Ca)Cu_2(SO_4)_8 \text{(Ca-bearing petrovite)},$$

and, as we can now assume for the intermediate members of the dobrovolskyite $Na_4Ca(SO_4)_3$ – cuprodobrovolskyite $Na_4Cu(SO_4)_3$ series:

$$0.5Na_2Cu(SO_4)_2 \text{ (saranchinaite)} + 1.5Na_2SO_4 \text{ (metathénardite)} + 0.5CaSO_4 \rightarrow Na_4Cu_{0.5}Ca_{0.5}(SO_4)_3 \text{ (cuprodobrovolskyite)}.$$

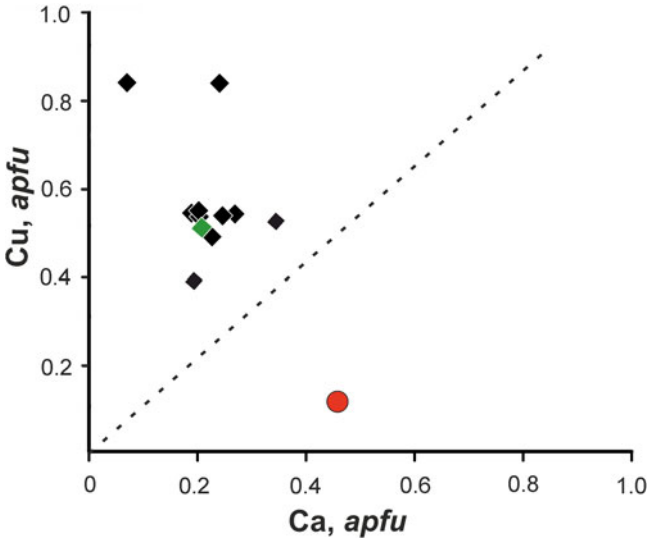

Figure 10. The Ca:Cu ratio (formula based on 12 O apfu) in cuprodobrovolskyite (diamonds) and the holotype dobrovolskyite (Shablinskii *et al.*, 2021) (red circle). The composition of the cuprodobrovolskyite sample with the studied crystal structure is marked as a green diamond. The dotted line shows the formal border between dobrovolskyite and cuprodobrovolskyite.

The indirect evidence of the high-temperature origin of cuprodobrovolskyite (and probably dobrovolskyite) follows from the results of the experiments aimed at synthesis of petrovite reported by Shorets (2022) who used the mixture of Na_2SO_4, $CaSO_4$ and $CuSO_4$ in ratios of 5:1:1, pressed this mixture in tablets and then heated the tablets at $T = 600$°C for 60 h. However, instead of the expected petrovite, the main phase formed in this experiment was a Cu-bearing variety of dobrovolskyite with tenorite admixture (Shorets, 2022).

Our heating experiment shows the sample studied, with the assemblage of cuprodobrovolskyite, petrovite and saranchinaite, partly decomposed with segregation of CuO on the crucible walls. Among the mentioned sulfates only cuprodobrovolskyite stays stable after heating, as was confirmed by the powder X-ray diffraction (Fig. 6). This demonstrates that cuprodobrovolskyite can be assumed as the most high-temperature phase in comparison with saranchinaite and petrovite. The appearance of cuprodobrovolskyite in the high-temperature fumarolic mineral association could be due to the heating of initial kröhnkite – a supergene mineral formed in winter in the upper part of this fumarole system and its subsequent transformations as a result of the interactions between abundant alkali-copper sulfates (euchlorine, wulffite, etc.) with atmospheric water and water vapour.

We believe, cuprodobrovolskyite forms at temperatures higher than 400°C whereas saranchinaite and petrovite seem to be more low-temperature sulfates which can appear, in particular, as products of transformations of cuprodobrovolskyite after cooling. As was shown by us (Shchipalkina *et al.*, 2021, 2023a), different types of exsolution and other solid-state transformations are typical for high-temperature Na-rich sulfates with aphthitalite-related structures in fumarolic systems. Generally, data on structure-superstructure relationships between aphthitalite-like crystal structures, the occurrence of cuprodobrovolskyite, and its relationship with other sulfates, allow us to propose cuprodobrovolskyite being a high-temperature phase (possibly quenched) with ordered univalent (Na) and bivalent (Cu, Ca) cations.

Acknowledgements. We are grateful to Andrey Yu. Bychkov for his help with heating experiments. We thank anonymous referees for their valuable comments. The mineralogical and structural studies of cuprodobrovolskyite and crystal chemical analysis by NVS, IVP and NVZ were supported by the Russian Science Foundation, grant no. 19-17-00050. The technical support by the SPbSU X-Ray Diffraction Resource Center in the powder XRD study is acknowledged.

Supplementary material. The supplementary material for this article can be found at https://doi.org/10.1180/mgm.2023.85.

Competing interests. The authors declare none.

References

Balassone P., Panikorovskii T.L., Pellino A., Bazai A.V., Bocharov V.N., Goychuk O.F., Avdontseva E.Y., Yakovenchuk V.N., Krivovichev S.V., Petti C., Cappelletti P., Mondillo N., Moliterni A. and Altomare A. (2023) Enricofrancoite, IMA 2023-002. CNMNC Newsletter 74. *Mineralogical Magazine*, **87**, 783–787.

Borisov A.S., Siidra O.I., Kovrugin V.M., Golovin A.A., Depmeier W., Nazarchuk E.V. and Holzheid A. (2021) Expanding the family of mineral-like anhydrous alkali copper sulfate framework structures: new phases, topological analysis and evaluation of ion migration potentialities. *Journal of Applied Crystallography*, **54**, 237–250.

Britvin S.N., Dolivo-Dobrovolsky D.V. and Krzhizhanovskaya M.G. (2017) Software for processing the X-ray powder diffraction data obtained from the curved image plate detector of Rigaku RAXIS Rapid II diffractometer.

Zapiski Rossiiskogo Mineralogicheskogo Obshchestva, **146**, 104–107 [in Russian].

Filatov S.K., Shablinskii A.P., Vergasova L.P., Saprikina O.Y., Bubnova R.S., Moskaleva S.V. and Belousov A.B. (2019) Belomarinaite $KNa(SO_4)$: A new sulphate from 2012–2013 Tolbachik Fissure Eruption, Kamchatka Peninsula, Russia. *Mineralogical Magazine*, **83**, 569–575.

Filatov S.K., Shablinskii A.P., Krivovichev S.V., Vergasova L.P. and Moskaleva S.V. (2020) Petrovite, $Na_{10}CaCu_2(SO_4)_8$, a new fumarolic sulfate from the Great Tolbachik fissure eruption, Kamchatka Peninsula, Russia. *Mineralogical Magazine*, **84**, 691–698.

Fischmeister H.F. (1962) Röntgenkristallographische Ausdehnungsmessungen an einigen Alkalisulfaten. *Monatshefte für Chemie*, **93**, 420–434.

Gorelova L.A., Vergasova L.P., Krivovichev S.V., Avdontseva E.Y., Moskaleva S.V., Karpov G.A. and Filatov S.K. (2016) Bubnovaite, $K_2Na_8Ca(SO_4)_6$, a new mineral species with modular structure from the Tolbachik volcano, Kamchatka peninsula, Russia. *European Journal of Mineralogy*, **28**, 677–686.

Guo J., Liang Y., Song R., Loh J.Y.Y., Kherani N.P., Wang W., Kubel C., Dai Y., Wang L. and Ozin G.A. (2021) Construction of new active sites: cu substitution enabled surface frustrated lewis pairs over calcium hydroxyapatite for CO_2 hydrogenation. *Advanced Science*, **8**, Paper 2101382.

Hatert F. (2019) A new nomenclature scheme for the alluaudite supergroup. *European Journal of Mineralogy*, **31**, 807–822.

Ibers J.A. and Hamilton W.C. (1974) *International Tables for X-ray Crystallography: Revised and Supplementary Tables*. Kynoch Press, Birmingham, UK.

Kosek F., Culka A. and Jehlicka J. (2018) Raman spectroscopic study of six synthetic anhydrous sulfates relevant to the mineralogy of fumaroles. *Journal of Raman Spectroscopy*, **49**, 1205–1216.

Kovrugin V.M., Nekrasova D.O., Siidra O.I., Mentre O., Masquelier C., Stefanovich S. Yu. and Colmont M. (2019) Mineral-inspired crystal growth and physical properties of Na_2 $Cu(SO_4)_2$ and review of $Na_2M(SO_4)_2(H_2O)_x$ ($x = 0$–6) compounds. *Crystal Growth & Design*, **19**, 1233–1244.

Nakamoto K. (1986) *Infrared and Raman Spectra of Inorganic and Coordination Compounds*. John Wiley & Sons, New York.

Pekov I.V., Koshlyakova N.N., Zubkova N.V., Lykova I.S., Britvin S.N., Yapaskurt V.O., Agakhanov A.A., Schipalkina N.V., Turchkova A.G. and Sidorov E.G. (2018) Fumarolic arsenates – a special type of arsenic mineralization. *European Journal of Mineralogy*, **30**, 305–322.

Pekov I.V., Shchipalkina N.V., Zubkova N.V., Gurzhiy V.V., Agakhanov A.A., Belakovskiy D.I., Chukanov N.V., Lykova I.S., Vigasina M.F., Koshlyakova N.N., Sidorov E.G. and Giester, G. (2019) Alkali sulfates with aphthitalite-like structures from fumaroles of the Tolbachik volcano, Kamchatka, Russia. I. Metathénardite, a natural high-temperature modification of Na_2SO_4. *The Canadian Mineralogist*, **57**, 885–901.

Petříček V., Dušek M. and Palatinus L. (2014) Crystallographic Computing System JANA2006: General features. *Zeitschrift für Kristallographie*, **229**, 345–352.

Rasmussen, S.E., Jorgensen, J.E. and Lundtoft, B. (1996) Structures and phase transitions of Na_2SO_4. *Journal of Applied Crystallography*, **29**, 42–47.

Ruck K., Wolf M., Ruck M., Eckert D., Krabbes, G. and Müller K.H. (2001) "$CaCu_2O_3$" – a nonstoichiometric compound: structural disorder and magnetic properties. *Materials Research Bulletin*, **36**, 1995–2002

Shablinskii A.P., Filatov S.K., Krivovichev S.V., Vergasova L.P., Moskaleva S.V., Avdontseva E.Y., Knyazev A.V. and Bubnova R.S. (2021) Dobrovolskyite, $Na_4Ca(SO_4)_3$, a new fumarolic sulfate from the Great Tolbachik fissure eruption, Kamchatka Peninsula, Russia. *Mineralogical Magazine*, **85**, 233–241.

Shannon R.D. and Prewitt C.T. (1969) Effective ionic radii in oxides and fluorides. *Acta Crystallographica Section B*, **25**, 925–946

Shchipalkina N.V., Pekov I.V., Chukanov N.V., Belakovskiy D., Zubkova N.V., Koshlyakova N.N., Britvin S.N. and Sidorov E.G. (2020a) Alkali sulfates with aphthitalite-like structures from fumaroles of the Tolbachik volcano, Kamchatka, Russia. II. A new mineral, natroaphthitalite, and new data on belomarinaite. *The Canadian Mineralogist*, **58**, 167–181.

Shchipalkina N.V., Pekov I.V., Koshlyakova N.N., Britvin S.N., Zubkova N.V., Varlamov D.A. and Sidorov E.G. (2020b) Unusual silicate mineralization in fumarolic sublimates of the Tolbachik volcano, Kamchatka, Russia–Part 1: Neso-, cyclo-, ino-and phyllosilicates. *European Journal of Mineralogy*, **32**, 101–119.

Shchipalkina N.V., Pekov I.V., Britvin S.N., Koshlyakova N.N. and Sidorov E.G. (2021) Alkali sulfates with aphthitalite-like structures from fumaroles of the Tolbachik volcano, Kamchatka, Russia. III. Solid solutions and exsolution. *The Canadian Mineralogist*, **59**, 713–727.

Shchipalkina N.V., Koshlyakova N.N., Pekov I.V., Agakhanov A.A., Britvin S.N. and Nazarova M.A. (2023a) Alkali sulfates with aphthitalite-like structures from fumaroles of the Tolbachik volcano, Kamchatka, Russia. IV. Aphthitalite–palmierite regular intergrowths: crystallography, chemistry and genesis. *The Canadian Journal of Mineralogy and Petrology*, **61**, 609–622.

Shchipalkina N.V., Pekov I.V., Koshlyakova N.N., Belakovskiy D.I., Zubkova N.V., Agakhanov A.A., Britvin S.N., and Nazarova M.A. (2023b) Cuprodobrovolskyite, IMA 2022-061. CNMNC Newsletter 70. *Mineralogical Magazine*, **87**, https://doi.org/10.1180/mgm.2022.135.

Shi N., Sanson A., Venier A., Fan L., Sun C., Xing X. and Chen J. (2020) Negative and zero thermal expansion in α-$(Cu_{2-x}Zn_x)V_2O_7$ solid solutions. *Chemical Communications*, **56**, 10666–10669.

Shorets O.Y. (2022) *Thermal Expansion and Phase Transformations of Exhalation Sulfates of Alkali Metals – Minerals of the Tolbachik Volcano (Kamchatka Peninsula) and Their Synthetic Analogues*. PhD thesis. St. Petersburg University, Russia.

Siidra O.I., Nazarchuk E.V., Zaitsev A.N., Lukina E.A., Avdontseva E.Y., Vergasova L.P., Vlasenko N.S., Filatov, S.K., Turner R. and Karpov G.A. (2017) Copper oxosulfates from fumaroles of Tolbachik volcano: puninite $Na_2Cu_3O(SO_4)_3$ – a new mineral species and structure refinements of kamchatkite and alumoklyuchevskite. *European Journal of Mineralogy*, **29**, 499–510.

Siidra O.I., Lukina E.A., Nazarchuk E.V., Depmeier W., Bubnova R.S., Agakhanov A.A., Avdontseva E.Y., Filatov S.K. and Kovrugin V.M. (2018) Saranchinaite, $Na_2Cu(SO_4)_2$, a new exhalative mineral from Tolbachik volcano, Kamchatka, Russia, and a product of the reversible dehydration of kröhnkite, $Na_2Cu(SO_4)_2(H_2O)_2$. *Mineralogical Magazine*, **82**, 257–274.

Siidra O.I., Borisov A.S., Charkin D.O., Depmeier W. and Platonova N.V. (2021a) Evolution of fumarolic anhydrous copper sulfate minerals during successive hydration/dehydration. *Mineralogical Magazine*, **85**, 1–16.

Siidra O.I., Charkin D.O., Kovrugin V.M. and Borisov A.S. (2021b) K(Na,K) $Na_2[Cu_2(SO_4)_4]$: a new highly porous anhydrous sulfate and evaluation of possible ion migration pathways. *Acta Crystallographica*, B77, 1003–1011.

Siidra O.I., Nekrasova D.O., Charkin D.O., Zaitsev A.N., Borisov A.S., Colmont M., Mentre O. and Spiridonova D. (2021c) Anhydrous alkali copper sulfates – a promising playground for new Cu^{2+} oxide complexes: new Rb-analogues of fumarolic minerals. *Mineralogical Magazine*, **85**, 831–845.

Singh S. Neveu A., Jayanthi K., Das T., Chakraborty S., Navrotsky A., Pralong V. and Barpanda P. (2022) Facile synthesis and phase stability of Cu-based $Na_2Cu(SO_4)_2{\cdot}xH_2O$ ($x = 0$–2) sulfate minerals as conversion type battery electrodes. *Dalton Transactions*, **51**, 11169–11179.

Ulutagay-Kartin M., Etheredge K.M.S.G., Schimek G.L. and Hwu S.-J. (2002) Synthesis, structure, and magnetic properties of two quasi-low-dimensional antiferromagnets, $NaMnAsO_4$ and β-$NaCuPO_4$. *Journal of Alloys and Compounds*, **338**, 80–86.

Warr L.N. (2021) IMA-CNMNC approved minerals symbols. *Mineralogical Magazine*, **85**, 291–320.

https://doi.org/10.1180/mgm.2023.85 Published online by Cambridge University Press